Toxicology in Vitro 61 (2019) 104614

Contents lists available at ScienceDirect

Toxicology in Vitro

journal homepage: www.elsevier.com/locate/toxinvit

Higginsianins A and B, two fungal diterpenoid α-pyrones with cytotoxic activity against human cancer cells

Felicia Sangermano[a], Marco Masi[b], Maria Vivo[a], Peravali Ravindra[c], Alessio Cimmino[b], Alessandra Pollice[a], Antonio Evidente[b], Viola Calabrò[a,*]

[a] Department of Biology, University of Naples Federico II, Via Cintia 4, 80126 Naples, Italy
[b] Department of Chemical Sciences, University of Naples Federico II, Via Cintia 4, 80126 Naples, Italy
[c] Institute of Toxicology and Genetics (ITG), Karlsruhe Institute of Technology, Karlsruhe, Germany

ARTICLE INFO

Keywords:
Colletotrichum higginsianum
Higginsianins
Cancer cells
Cell cycle arrest
Anticancer metabolites
Cell death

ABSTRACT

Two new diterpenoid α-pyrones, named higginsianins A and B, were isolated from the mycelium of the microbial fungus *Colletotrichum higginsianum* grown in liquid culture. In previous studies, we have shown that both compounds reduce viability of different types of cancer cells in culture. Here, we extend our previous observations and explore, at a deeper level, the cellular effects of higginsianins treatment. Higginisianins A and B reduce viability of A431, HeLa and H1299 cancer cells. Both compounds increase the level of the cell cycle inhibitor p21WAF and reduce the rate of cell proliferation. Cell cycle analyses reveal that higginsianins arrest cancer cells in S-phase. Furthermore, cells incubated with higginsianins reveal discrete γ-H2AX positive nuclear foci indicating the occurrence of DNA lesions. At longer incubation times, higginsianins induce massive cell detachment and non-apoptotic cell death. Human primary keratinocytes and spontaneously immortalized Hacat cells, a preneoplastic cell line model, are less sensitive to higginsianins effects. These findings suggest that higginsianins exhibit considerable cytotoxicity against a wide spectrum of malignant cells and may be considered as promising anticancer agents.

1. Introduction

Nature is an attractive source of new therapeutic candidate compounds as potential anti-cancer agents (Bhanot et al., 2011). Microbial fungi produce a plethora of secondary metabolites belonging to all the classes of natural compounds. Fungal metabolites are also well known as phytotoxins with potential application in agriculture as bioherbicides (Cimmino et al., 2015; Masi et al., 2019) or in medicine as anticancer compounds (Evidente et al., 2014).

The genus *Colletotrichum* is considered one of the most dangerous in agriculture including a large number of fungal plant pathogens responsible for severe diseases to many cultivated plants. It is also well known for its ability to synthesize a wide array of secondary metabolites having various biological properties that can be exploited for biotechnological applications (Garcia-Pajon and Isidro, 2003).

During a screening carried out on several *Colletotrichum* species aimed to find out sources of novel natural metabolites and/or biological activities, two fungi were selected for their interesting biological properties, namely *Colletotrichum gleosporioides* and *Colletotrichum higginsianum*.

The culture filtrates of *C. gleosporioides* showed a very interesting phytotoxic activity against *Ambrosia artemisiifolia L.*, the worldwide spread plant responsible for severe human allergies. In fact, from *C. gleosporioides* culture filtrates three phytotoxic metabolites were isolated and identified as colletochlorin A, orcinol and tyrosol with the first one that induced large necrosis when assayed by leaf-punture assay on *A. artemisifolia* (Masi et al., 2018).

From the mycelium of *C. higginsianum,* instead, two new diterpenoid α-pyrones, named higginsianins A (Higg A) and B (Higg B) (Fig. 1), were firstly isolated. Diterpenoid α-pyrones have previously been reported to have immunosuppressive properties (Lim et al., 2015). However, recent studies indicated that Higgs A and B reduce cancer cell viability (Cimmino et al., 2016) and prompted a deeper study to investigate the potential of these two diterpenoid α-pyrones against cancer cells.

Tumors of any given cell type may show a wide range of difference in structure and properties and are characterized by molecular and functional heterogeneity. Here, we show molecular evidence that Higgs A and B have cytotoxic activity against several types of human cancer cell lines.

* Corresponding author.
E-mail address: viola.calabro@unina.it (V. Calabrò).

https://doi.org/10.1016/j.tiv.2019.104614
Received 30 April 2019; Received in revised form 12 July 2019; Accepted 28 July 2019
Available online 03 August 2019

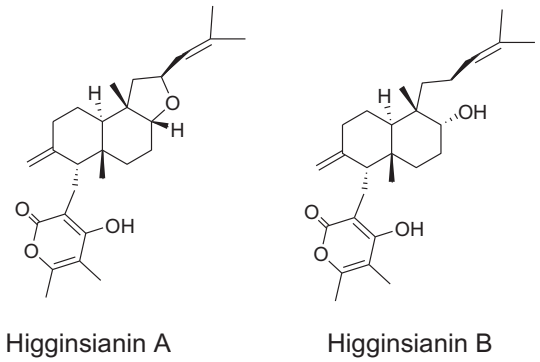

Fig. 1. *The structures of higginsianins A and B.*

2. Materials and methods

2.1. General

Optical rotations were measured in a $CHCl_3$ solution on a Jasco P-1010 digital polarimeter (Tokyo, Japan). ^1H and ^{13}C NMR spectra were recorded at 400/100 MHz in $CDCl_3$ on Bruker spectrometers (Karlsruhe, Germany). The same solvent was used as internal standard. LC/MS analyses were performed using the LC/MS TOF system (AGILENT 6230B, HPLC 1260 Infinity, Milan, Italy) Analytical and preparative TLC were performed on silica gel (Merck, Kieselgel 60, F_{254}, 0.25 and 0.5 mm, respectively, Darmstadt, Germany) or on reverse phase (Whatman, RP-18 F_{254}, 0.20 mm, Maidstone, UK) plates; the spots were visualized by exposure to UV light and/or iodine vapors and/or by spraying first with 10% H_2SO_4 in MeOH and then with 5% phosphomolybdic acid in EtOH followed by heating at 110 °C for 10 min. Column chomatography was performed using silica gel (Merck, Kieselgel 60, 0.063–0.200 mm).

2.2. Production, purification of higginsianins A and B

Higginsianins A and B were isolated by the fungus *C. higginsianum* grown on M1D medium as previously reported (Cimmino et al., 2016), The mycelium, recovered from the culture filtrates, was extracted with EtOAc and the corresponding organic extract fractionated by column and TLC chromatography to obtain higginsianins A and B as crystals and homogeneous solid as detailed previously (Cimmino et al., 2016). Higginsianins A and B were dissolved in DMSO and used at the indicated final concentrations and times.

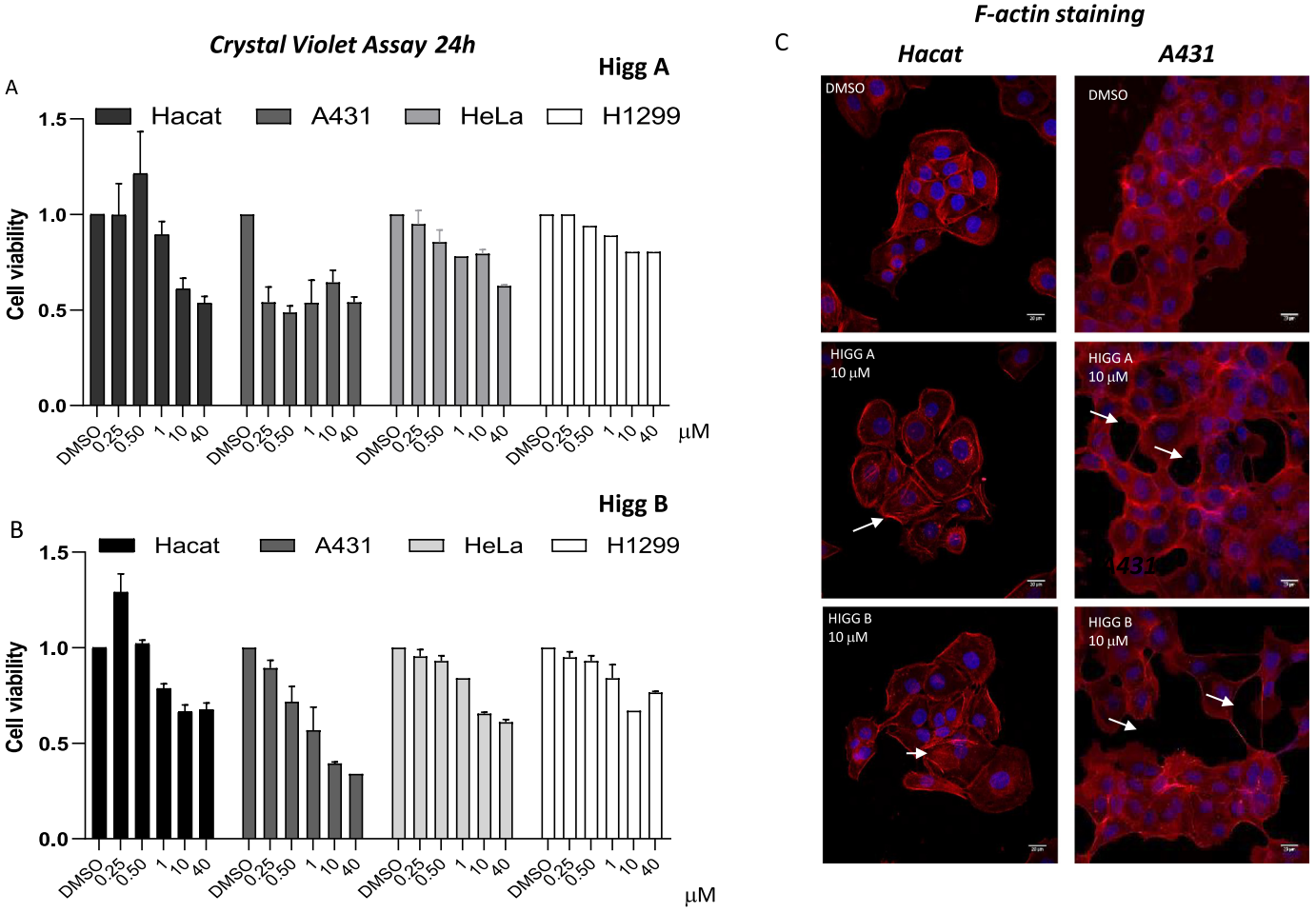

Fig. 2. *Crystal violet assay (CVA)*, Hacat, HeLa, H1299 and A431 cells were treated with different concentrations (0.25–40 uM) of Higg A (2A) or B (2B) for 24 h. As a control, cells were treated with an equal amount of DMSO in the absence of higginsianins. Cells were washed, fixed and stained with crystal violet. Upon solubilization, the amount of dye taken up by the monolayer was read at 570 nm for quantitation. Values shown in the plot are mean ± SE of three independent experiments. 2.C *F-actin staining*, cells were allowed to adhere onto coverslips for 24 h and then treated with 1 μM and 10 μM Higg A or B for 24 h, fixed and subjected to TRITC-conjugated phalloidin and DAPI staining to visualize actin cytoskeleton and nuclei. Representative images are shown. Images were taken with a Zeiss confocal laser-scanning microscope Axio Observer (scale bar, 20 μm). A 40 × objective was used and image analysis was performed using ImageJ. All the images were taken with the same setting. (For interpretation of the references to colour in this figure legend, the reader is referred to the web version of this article.)

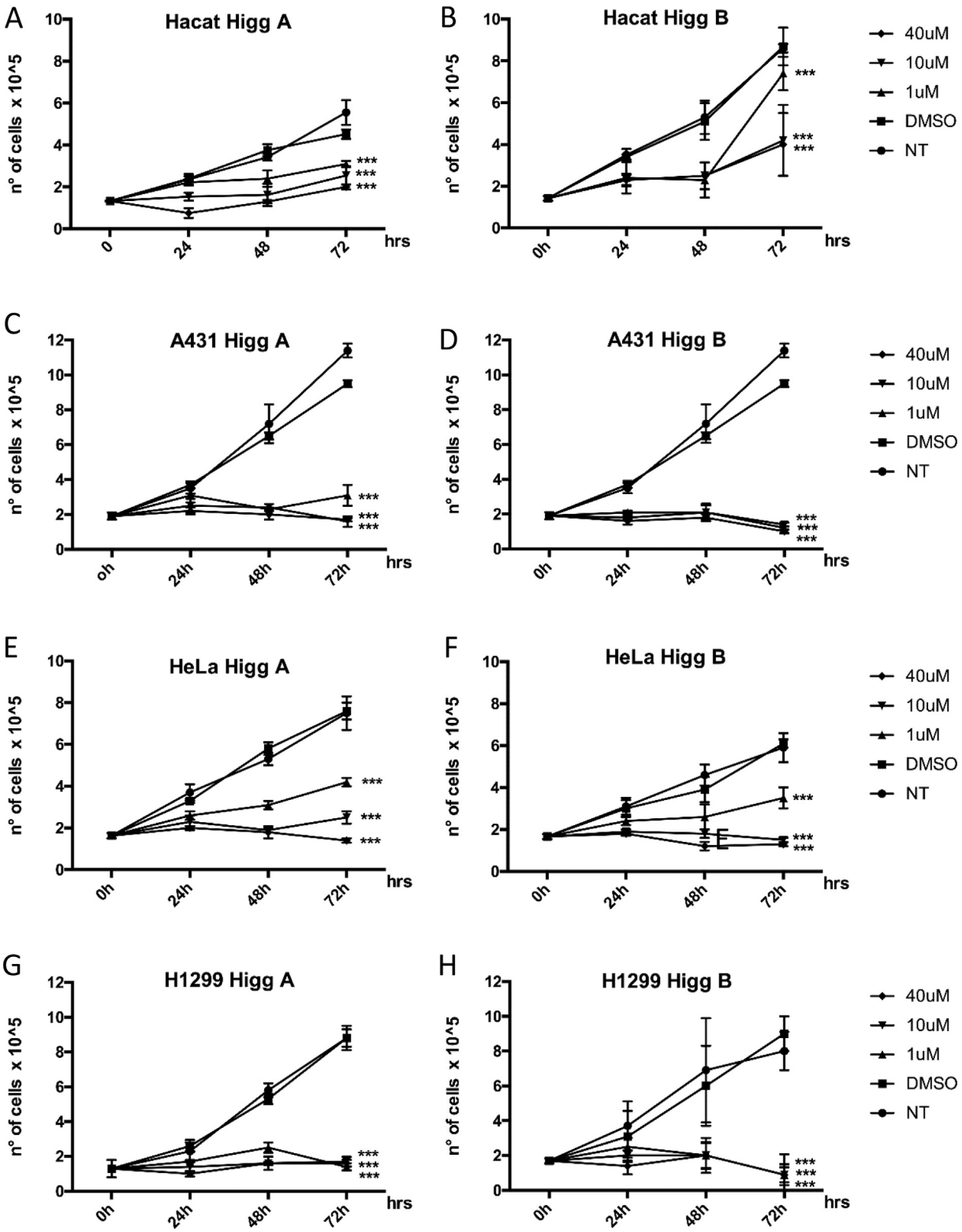

Fig. 3. *Effect of higginsianins on the rate of cell proliferation.* Hacat, A431, HeLa and H1299 cells were plated in DMEM with serum. Twenty-four hours later, the medium was changed and supplemented with 1, 10 or 40 μM higginsianins A or B in DMSO. The cells were counted on days 1, 2, and 3. Untreated cells (NT) or cells treated with DMSO alone were used as control. Values shown in the plot are mean ± SD of triplicate determinations. Asterisks represent significant results at $p = .05$.

2.3. Cell culture and reagents

Human Epidermal Keratinocytes NHEK-neo (# 0019290 Lonza Group, Basel Switzerland) were grown in KGMTN Gold keratinocyte Growth Medium BulletKitTM (# 00192060). Hacat, spontaneously immortalized keratinocytes from adult skin were purchased from Service Cell Line (CLS, Germany) and cultured as described (Amoresano et al., 2010; Vivo et al., 2009). HeLa cervical cancer cells (CCL-2),

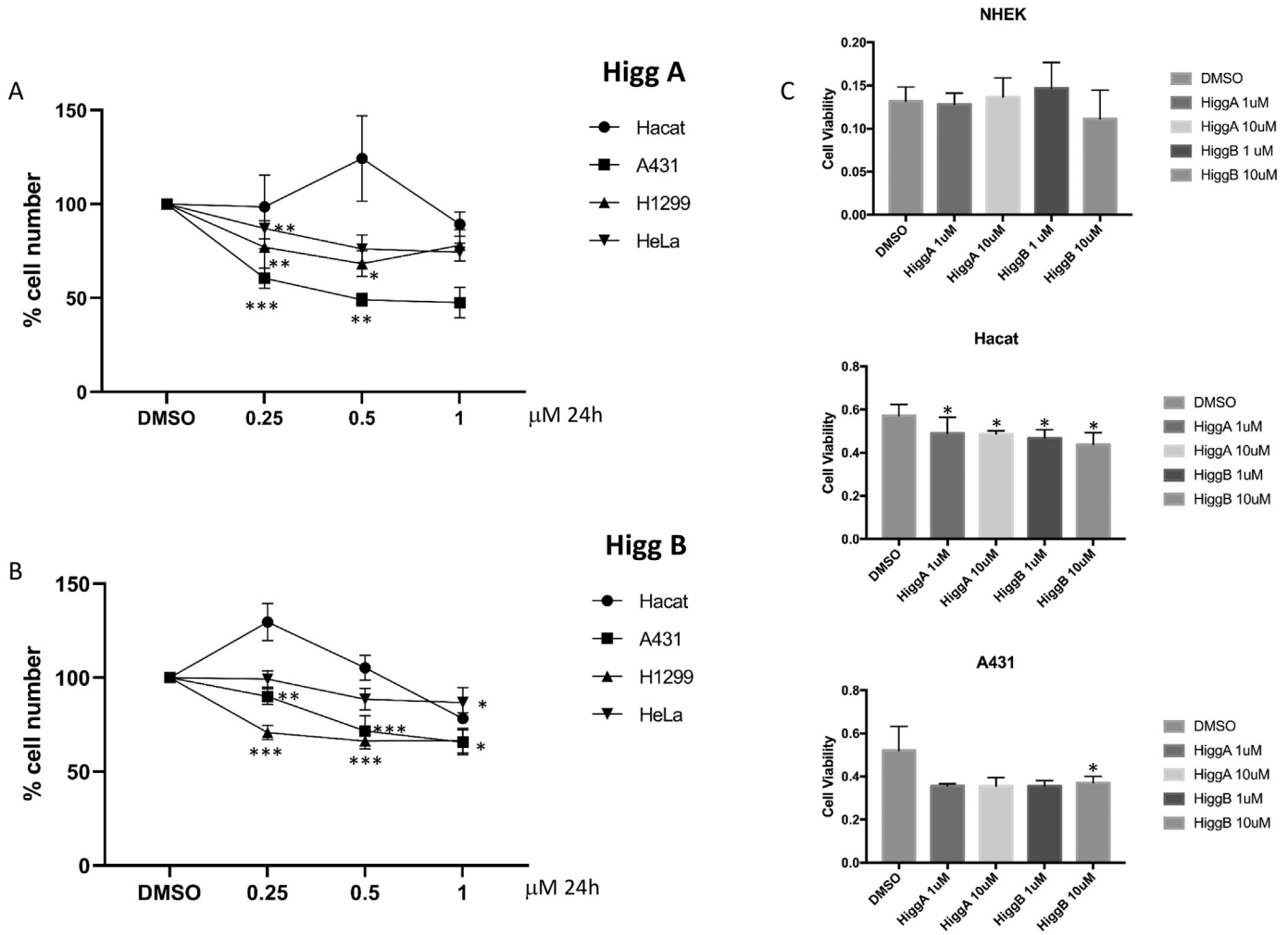

Fig. 4. *Effect of lower doses of higginsianins*. A, B. Hacat, A431, HeLa and H1299 cells were plated in DMEM with serum. Twenty-four hours later, the seeding medium was changed and supplemented with 0.25, 0.5 or 1 µM Higg A or B in DMSO. The cells were counted after 24 h of treatment. C. The effect of Higginsianins A and B on primary Keratinocytes, Hacat and A431 cells. The cells indicated above were seeded in DMEM and treated 24 h hours later with 1 µM HiggA and HiggB. Cell viability was measured by MTT assays. Values shown in the plot are mean ± SD of triplicate determinations. Asterisks represent significant results at p = .05.

H1299 (CRL-5803) human non-small cell lung carcinoma and A431 (ATCC-CRL1555) human epidermoid carcinoma cells were from American Type Culture Collection (ATCC, Manassas, VA). According to the p53 compendium database (http://p53.fr/tp53-database/the-tp53-cell-line-compendium), Hacat cells contain mutant p53 (H179Y/R282W), HeLa have p53 impaired function by viral infection, H1299 are p53 null while A431 contain only one p53 mutated allele (R273H). All mentioned cell lines were cultured in Dulbecco's Modified Eagle's Medium (DMEM, Sigma Chemical Co, St. Louis, MO, USA) supplemented with 10% fetal bovine serum (FBS, Hyclone Laboratories, Inc. Logan, UT, USA) at 37 °C in humified atmosphere of 5% CO2. All cell lines were routinely tested for mycoplasma contamination and were not infected.

2.4. Crystal violet assay (CVA)

Hacat, HeLa, H1299 and A431 cells were plated (2×10^5) on a 60 mM culture dishes and treated with DMSO or increasing concentrations (0.25, 0.50, 1, 10 and 40 µM) of Higg A or Higg B for 24 h. After treatments, the culture medium was removed and cells were covered with 2 ml of fixing solution (10% methanol; 10% acetic acid in distilled H_2O). Cells were then stained with crystal violet solution (0.5% *w/v* crystal violet, 25% methanol in distilled H_2O) for 20 min at room temperature. The stain solution was removed and dishes were washed with water and air dried. Dead cells detach from the surface of the culture plate and are removed from viable cell population during washing steps. Upon solubilization, the amount of dye taken up by the cell monolayer was quantitated in a spectrophotometer by reading the absorbance at 570 nm.

2.5. Cell growth profile

Cells were seeded at 1×10^5 in 35 mm dishes and treated with Higg A or Higg B at 1, 10, 40 µM for 48 h. Cells were harvested by suspension in 0.025% trypsin in 0.02% EDTA solution. Cell counts were performed in triplicates using a Neubauer chamber by trypan blue dye exclusion. Briefly, 20 µl cell suspension was diluted 1:1 with 0.4% solution of trypan blue in phosphate saline buffer pH 7.2. Cell counting was carried out at 24 h intervals for 3 days.

2.6. MTT assay

Cells were seeded at 2×10^4 in 24 well plate and treated with Higg A or Higg B (1 and 10 mM) for 24 h. MTT solution 1:10 (stock solution 5 mg/ml) was added to each well and the absorbance was measured in dual wavelength mode (570 nm and 630 nm). The percentage of cell viability was calculated as follows: mean (A570-A630). Values shown in the plot are mean ± SD of triplicate determinations. Asterisks

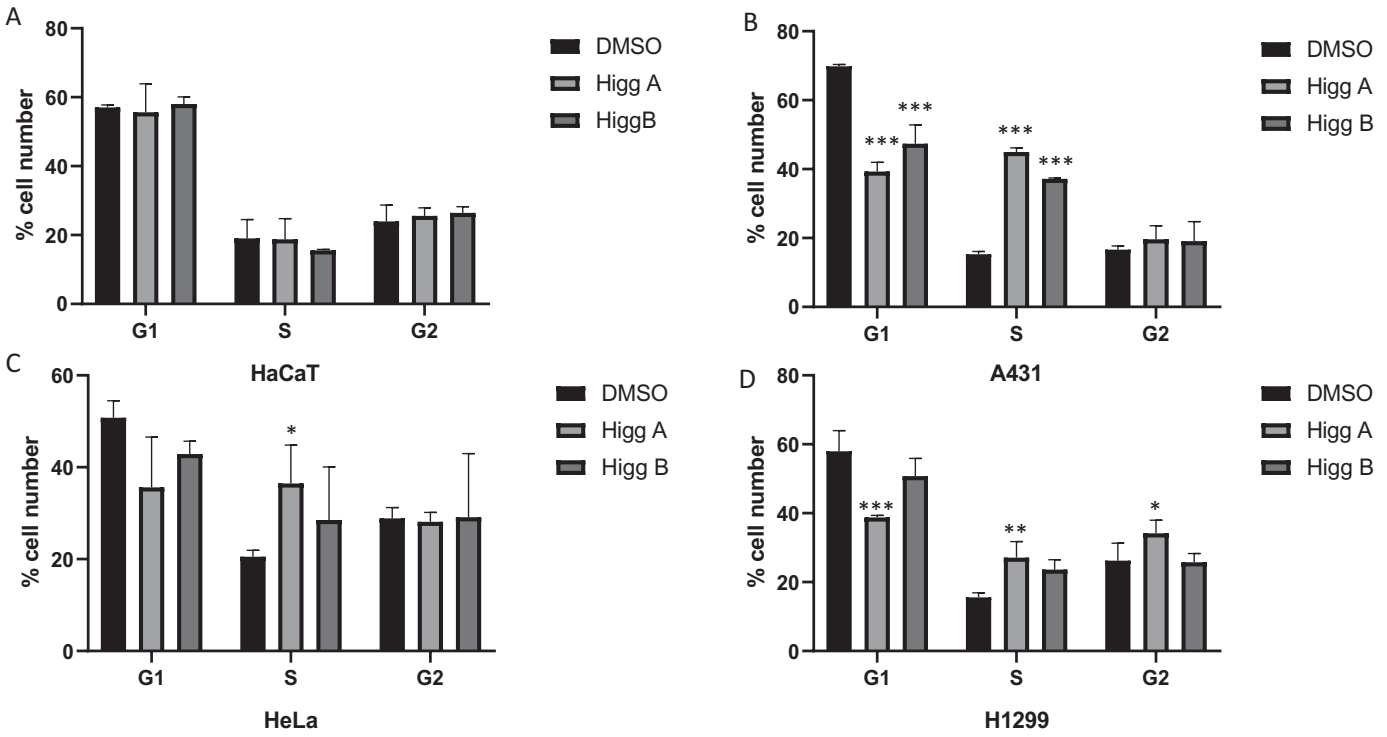

Fig. 5. *Cell cycle analysis*. Hacat, A431, HeLa and H1299 cells were treated with DMSO alone or 1 μM higginsianin A or B for 24 h. Cell cycle distribution was analyzed by flow cytometer. After treatment, cells were fixed and stained with a PI solution at a concentration of 50 μg/ml for 30 min at RT. Cell cycle analysis was performed by BD Accury™ C6 flow cytometer (BD Biosciences). Bars represent an average of 3 measurements. Error bars represent the means ± SD. Asterisks represent significant results at p = .05.

Table 1
Cell cycle analysis.

		DMSO			Higg A			Higg B		
		mean	sd	n	mean	sd	n	mean	sd	n
Hacat	G1	57,01	0,78	3	55,66	8,26	3	58,02	2,08	3
	S	19,0	5,52	3	18,78	5,96	3	15,54	0,27	3
	G2/M	23,98	4,74	3	25,57	2,31	3	26,45	1,82	3
A431	G1	69,85	0,50	3	39,29	2,66	3	47,36	5,49	3
	S	15,28	0,79	3	44,99	1,15	3	37,18	0,23	3
	G2/M	16,65	1,03	3	19,64	3,91	3	19,09	5,65	3
Hela	G1	50,79	3,67	3	35,64	10,93	3	42,89	2,76	3
	S	20,53	1,40	3	36,48	8,36	3	28,53	11,56	3
	G2/M	28,88	2,33	3	28,15	2,04	3	29,10	13,85	3
H1299	G1	57,95	6,03	3	38,78	0,58	3	50,79	5,11	3
	S	15,54	1,36	3	27,10	4,64	3	23,62	2,85	3
	G2/M	26,25	5,04	3	34,13	3,81	3	25,77	2,51	3

Flow cytometry data. Hacat, A431, HeLa and H1299 cells were treated with DMSO alone or 1 mM HiggA or B for 24 h. After treatment, cells were fixed and stained with propidium iodide as detailed in Materials and methods. The analysis was performed with a BD Accury™ C6 flow cytometer (BD Biosciences). Data shown in the plot are the means ± S.E of triplicates. Mean and standard deviation (sd) was calculated on biological triplicates (n) using GraphPad Prism 8 software. Significant results are shown in Fig. 2.

represent significant results at $p = .05$.

2.7. Cell cycle analysis

Cells were seeded at 3×10^5 in 35 mm dishes and treated with Higg A or Higg B (10 μM) for 24 h. Cells were then trypsinized and washed by centrifugation (12,000 rpm, 4 min, 4 °C) in Phosphate Buffered Saline (PBS 1×). The cell pellet was resuspended in ethanol, incubated in ice for 2 h and centrifuged at 12000 rpm, 5 min, 4 °C. After a wash in PBS, the cell pellet was incubated in PBS 1×, containing RNase 100 μg/ml for 20 min at RT. Propidium Iodide was then added at a concentration of 50 μg/ml for 30 min at RT. Cell cycle analysis was performed on the BD Accury™ C6 flow cytometer (BD Biosciences). Cell debris and aggregates were excluded from the analysis.

2.8. Western blot analysis

Western blot was performed as previously reported (di Martino et al., 2016; Vivo et al., 2015). Briefly, 25–30 μg of whole cell extracts were separated by SDS-PAGE, subjected to western blot and incubated overnight at 4 °C with antibodies. Antibodies against p21WAF, PARP1 and GAPDH were from Cell Signaling Technologies 9542, Boston, MA, USA. Each experiment was run in triplicate. Signal intensities of Western blot bands were quantified by Quantity One analysis software (Biorad Laboratories, UK) and analyzed by GraphPad Prism 8.0.2 software.

2.9. Immunofluorescence

Cells were seeded in 35 mm dish on micro cover glasses (BDH) and treated with Higgs A and B at 1 and 10 μM. At 24 h after treatment cells were washed with cold phosphate-buffered saline (PBS) and fixed with 4% paraformaldeide (Sigma-Aldrich, Germany) for 15 min at RT. Cells were permeabilized with ice-cold 0.5% Triton X-100 for 5 min and then washed with PBS. Cells were then incubated with tetramethylrhodamine-conjugated phalloidin for 30 min or phospho-histone H2A.X (Ser139) antibody (from Cell Signaling Technologies 9542, Boston, MA, USA), followed by DAPI (Sigma-Aldrich) for 3 min and washed with PBS/0.05% Tween. Coverslip were mounted with Ibidi mounting medium (Ibidi GmbH, Martinsried, Germany). Images were taken with a Zeiss confocal laser-scanning microscope Axio Observer (scale bar, 20 μm). A 40× objective was used and image analysis was performed using ImageJ. All the images were taken with the same setting (Vivo et al., 2017).

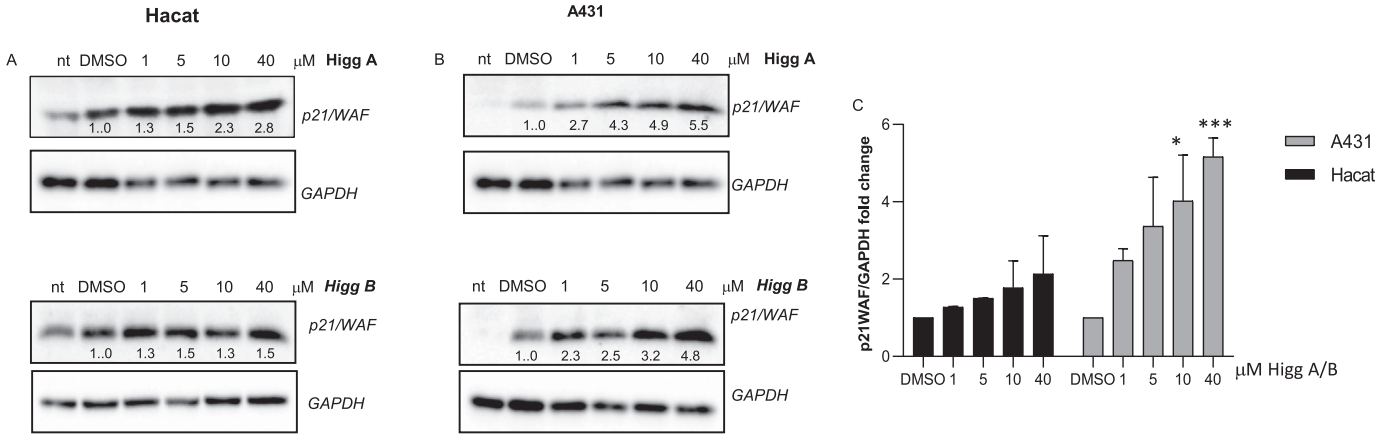

Fig. 6. *Effect of higginsianins on the p21WAF protein level.* Representative immunoblots showing the effects of higginsianins on p21WAF expression in Hacat (A) and A431 (B) cells. Cells were incubated for 48 h with the indicated concentrations (1–40 µM) of Higg A or Higg B. Proteins were separated on 15% SDS-polyacrylamide gel (25 µg/lane) and transferred to PVDF membranes. The level of p21WAF protein was analyzed *via* Western blotting with mouse monoclonal antibodies. The blots were then re-probed with anti-GAPDH antibody, to confirm an equal amount of protein loading. The signals intensities, indicated by numbers, were quantitated by ImageLab software and expressed as the rate between p21WAF and GAPDH (Fig. 6C, bar graphs). Asterisks represent significant results at $p < .001$ (***).

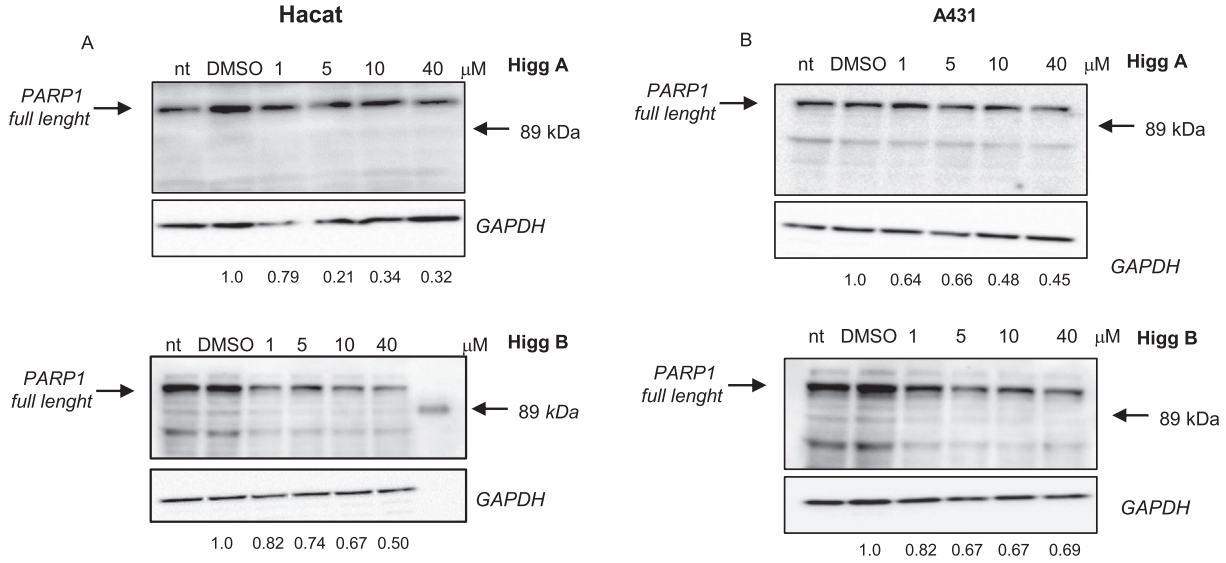

Fig. 7. *Effect of Higg A and B on PARP1 protein level* in Hacat (Fig. 7A) and A431 cells (Fig. 7B). Representative immunoblots showing the effects of higginsianins on the PARP1 protein level. Proteins were separated on 10% SDS-polyacrylamide gel (25 µg/lane) and transferred to PVDF membranes. Protein bands were revealed with antibodies directed against full length (113 kDa) and cleaved PARP1 (89 kDa). The blots were then re-probed with anti-GAPDH antibody, to confirm an equal amount of protein loading. The signals intensity was quantitated by ImageLab software and expressed as the rate between PARP1 and GAPDH signals as indicated by the numbers.

2.10. Statistical analysis

Statistical analyses were carried out using the GraphPad Prism 8 software. Data were represented as the mean ± standard deviation and analyzed for statistical significance using ordinary one-way or two-ways analysis of variance (ANOVA) and multiple comparisons. For all test, $P < .5$ was considered to indicate a statistically significant difference.

2.11. Transfection

Trypsinized cells were transfected using 1 µg of CMV or p53 plasmid DNA by electroporation with Neon Transfection System Invitrogen (1005 Voltage, 35 Width, 2 pulses) and seeded in 24 well at confluence $2{,}5 \times 10^4$ each well. After 24 h cells were treated with Higg A or Higg B (1 µM) for 24 h. MTT solution 1:10 (stock solution 5 mg/ml) was added to each well and the absorbance was measured in dual wavelength mode (570 nm and 630 nm). The percentage of cell viability was calculated as follows: mean (A570-A630). Values shown in the plot are mean ± SD of triplicate determinations. Asterisks represent significant results at $p = .05$.

3. Results

3.1. Higginsianins A and B isolation

Higginsianins A and B (Fig. 1) were isolated from the mycelium of *C. higginsianum* and their identity and purity were ascertained by comparison with the previously reported chromatographic (TLC in different conditions), physic (specific optical rotation) and spectroscopic (^{1}H and ^{13}C NMR and ESI MS) data (Cimmino et al., 2016).

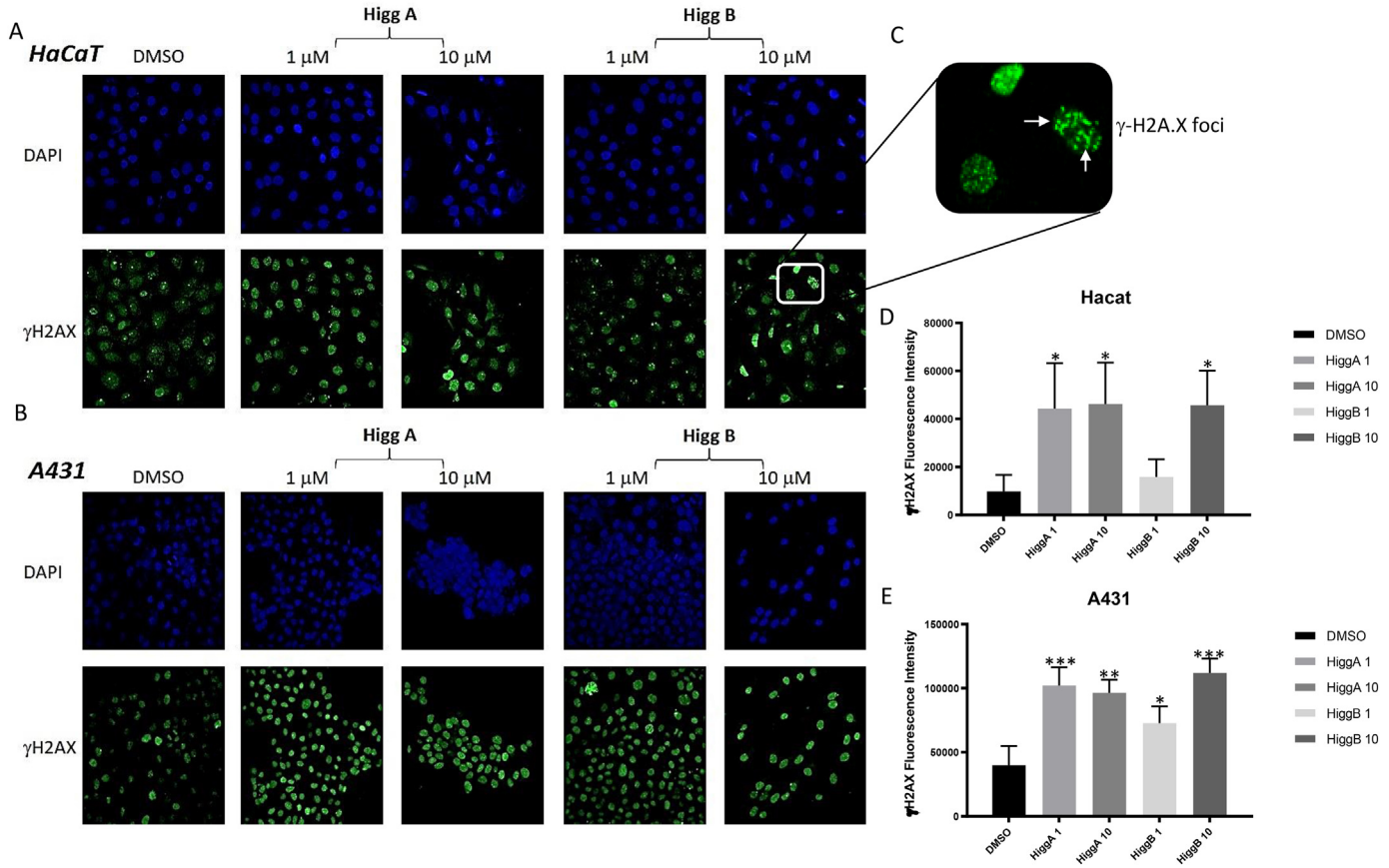

Fig. 8. Immunofluorescence microscopy showing γ-H2AX foci formation (green) in nuclei of Hacat (Fig. 8A) or A431 cells (Fig. 8B) treated for 24 h with DMSO alone, 1 or 10 μM Higgs A or B. Nuclei were stained with DAPI (blue). Note the highest number of γ-H2AX foci induced in A431 cells compared to Hacat cells. Images from 3 fields per each experimental point were collected to obtain data for up to 150 cells. Quantitation of γ-H2AX foci fluorescence was performed by Image J software and shown as mean ± SD in graph bars of panels D (Hacat) and E (A431) cells. Asterisks represent significant results at p = .05. (For interpretation of the references to colour in this figure legend, the reader is referred to the web version of this article.)

3.2. Higginsianins A and B cytotoxicity in human cancer cell lines

A preliminary evaluation of *in vitro* cytotoxic activity of Higgs A and B was performed by crystal violet dye-binding Assay (CVA) against A431, HeLa and H1299 human cancer cell lines. Spontaneously immortalized Hacat keratinocytes were used as a preneoplastic cell line model. As shown in Fig. 2A and B, after 24 h of treatment with increasing concentrations of higginsianins (from 0 to 40 μM), we noticed a reduction of the number of adherent cells in the culture plates compared to cells treated with DMSO alone. A431 cells were the most sensitive with a 50% reduction at 0.25 μM Higg A (Fig. 2A). However, at 1 μM both Higgs A and B were able to reduce the number of all tested cancer cell lines (Fig. 2A and B).

Moreover, given that higginsianin-treated cells rounded up and detached from the plate, we examined the F-actin cytoskeleton structure by fluorescence microscopy using tetramethylrhodamine-conjugated phalloidin. Treatments of Hacat cells with 1 or 10 μM Higgs A or B induced a flattened morphology and formation of stress fibers (Fig. 2C, left panel, white arrows). However, cells remain close to each other and adherent to the surface (Fig. 2C, left panel). A431 cells, instead, dramatically lose their cell-cell contacts resulting in empty holes clearly visible in the cell monolayer (Fig. 2C, right panel, white arrows).

To evaluate the dose and time-dependence cytotoxicity of higginsianins, we estimated the proliferation rate of cells treated with different concentrations, between 0 and 40 μM of Higg A or Higg B and incubation times (24, 48 and 72 h). After 24 h of incubation with Higg A or Higg B at concentration equal or higher than 1 μM, all cell lines underwent growth arrest (Fig. 3A–H).

At 48 h of incubation with 1, 10 or 40 μM Higg A or Higg B, A431 and H1299 cells get detached from the plate while Hacat cells were able to resume the growth (Fig. 3A and B). A similar behavior was observed in HeLa cells treated with 1 μM Higg A or Higg B (Fig. 3E and F).

Furthermore, we performed a cell count after 24 h of treatment with Higgs A or Higg B at concentrations lower than 1 μM (0.25 and 0.50 μM). Interestingly, while the number of Hacat cells was unaffected by Higg A and slightly reduced by Higg B (92% at 0.25 and 75% at 0.5 μM Higg B), the number of cancer-derived cells was significantly reduced by both higginsianins (Fig. 4A and B).

Finally, we tested the sensitivity of human primary keratinocytes to higginsianins treatment by comparing them with HaCaT and A431 cells. We performed MTT viability assay after treatment with 1 and 10 μM Higg A or B for 24 h. As shown in Fig. 4C, unlike immortalized and transformed cells, the primary keratinocytes were almost insensitive to higginsianin treatments.

Because of the profound inhibition of cell proliferation caused by higginsianins we wanted to analyze if alterations in the cell cycle occurred. The effect of higginsianins on cell cycle progression was analyzed by flow cytometry after 24 h of treatment with 1 μM Higgs A or B (Fig. 5 and Table 1). As shown in Fig. 5A and Table 1, the cell cycle distribution of Hacat cells was not significantly affected by both higginsianins except for a slight increase in G2/M phase (about 2%). Conversely, all cancer cell lines were dramatically arrested in S-phase (Fig. 5B, C and D). Indeed, after 24 h of treatment, the percentage of A431 cells in S phase raised from 19 to 45% with Higg A and to 37% with Higg B (Fig. 5B). Similarly, the percentage of H1299 cells in S phase raised from 16 to 27% and 24% with Higgs A and B, respectively

(Fig. 5D) while in HeLa cells the S phase cells raised from 21% to 36 and 29% with 1 μM Higgs A and B, respectively (Fig. 5C). The S phase cell cycle arrest was essentially at the expense of the G1 phase in all cell lines tested while the G2 phase was almost unaffected as in HeLa cells or slightly increased as in A431 and H1299 cells (Fig. 5).

3.3. HiggA and B induce p21WAF expression level

To explore at molecular level the mechanism of higginsianin-induced cell growth arrest, we examined by western blot analysis the expression of p21WAF protein in Hacat and A431 cells after the treatment with increasing concentrations of Higg A or Higg B. p21WAF is the cyclin-dependent CDK4 and CDK2 inhibitor that halt cell cycle progression in G1/S phase (Sherr and Roberts, 1999). As shown in Fig. 6 A and B we found a dose-dependent increase of p21WAF in both cell lines with either higginsianins. Interestingly, A431 cells exhibited a stronger induction of p21WAF compared to Hacat cells (Fig. 6C).

Next, we have monitored PARP1 specific cleavage to evaluate the occurrence of apoptosis in higginsianins-treated Hacat and A431 cells. During apoptosis, PARP1 proteolytic cleavage by caspase 3 results in the accumulation of a C-terminal 89 kDa fragment containing the catalytic domain (Soldani and Scovassi, 2002). The proteolysis of PARP1 renders the enzyme inactive and this further facilitates apoptotic cell death. Thus, the presence of a 89 kDa PARP1 fragment is considered to be a very reliable biomarker of apoptosis. Unlike p53-null H1299 (Slovackova et al., 2012), Hacat and A431 cells are known to be apoptosis proficient despite their p53 mutant status (Lee et al., 2005; Gulli et al., 1996). We examined the expression of PARP1 in Hacat and A431 after 24 h treatment with increasing doses, from 1 to 40 μM, of Higg A or Higg B by pooling floating and adherent cells and performing immunoblot analysis. As shown in Fig. 7A and B we didn't observe accumulation of cleaved PARP1 (89 kDa) thus indicating that cells were undergoing non-apoptotic cell death.

3.4. Detection of DNA damage by immunofluorescence

Detection of nuclear γ-H2A.X foci indirectly provide evidence of the occurrence of DNA double strand breaks (DSB) and/or DNA replication stress (Mejia-Ramirez et al., 2015; Gagou et al., 2010). Upon induction of a DNA double-strand break, the H2A.X histone becomes rapidly phosphorylated at Serine 139 to form gamma-H2AX [γH2AX; (Rogakou et al., 1998)]. This phosphorylation event is dynamic, complex, and depends on interactions between MDC1, H2AX, and ATM and other kinases to persist (Savic et al., 2009). This amplified response is easily detected using antibodies to γ-H2AX, manifesting discrete nuclear foci.

Given that higginsianins induces S-phase arrest we monitored formation of γ-H2AX foci by immunofluorescence. Hacat and A431 cells were treated with 1 and 10 μM Higg A and B for 24 h. As shown in Fig. 8A and B, higginsianin treatment caused a remarkable increase of nuclear γH2AX foci (Fig. 8C, white arrows). The level of γ-H2A.X-positive fluorescence intensity was significantly increased after treatment with Higg A or B (Fig. 8D and E). Interestingly, at the lower concentration tested (1 μM) Higg B appeared to be considerably less toxic in Hacat cells than in A431cancer cells (Fig. 8D and E). All together these data provide strong evidence that higginsianins treatment causes DNA lesions that are likely responsible for the observed S-phase cell cycle arrest.

4. Discussion

Isoprenoids have proven to have important antitumor activity (Barbero et al., 2018). Taxol and aphidicolin, among them, are produced by plants and fungi and appear to be the most representative among the diterpenes with antitumor activity (Hao et al., 2013).

Higginsianins A and B are two novel diterpenoid α-pyrones recently isolated from *C. higginsianum*. The structural difference between Higgs A and B lies in the region far from the main α-pyrone chromophore (Fig. 1) and their structure and relative and absolute configuration were previously determined (Cimmino et al., 2016). By performing MTT assays, both higginsianins were found to possess promising antiproliferative effects against six distinct cancer cell lines derived from oligodendroglioma, glioblastoma, melanoma, lung and breast cancer (Cimmino et al., 2016).

Here, we have extended previous investigation by evaluating the cytotoxic activity of higginsianins in immortalized and transformed epithelial cells. The panel of cell lines selected for this study included Hacat, A431 and HeLa cells which have mutant or viral inactivated p53 and H1299 cells which have the homozygous deletion of the p53 locus (Reiss et al., 1992). Our data indicate that both higginsianins can efficiently induce p53-independent non-apoptotic cell death and are highly toxic to all cancer cell lines in a dose and time-dependent manner.

Although the precise molecular mechanism of action of higginsianins has to be determined, the up-regulation of the CDK inhibitor p21WAF is likely responsible for the cytostatic activity of both higginsianins and suggests that it may be the primary target of action of both metabolites.

Interestingly, we have evidence that higginsianin-treated cancer cells arrest in S-phase and are unable to progress through the S-phase. S-phase marks a particularly vulnerable time for cells to cope with DNA damage. DNA lesions act as physical impediments to the replicative polymerases. The induction of γ-H2A.X foci in cells treated with higginsianins provided clear evidence of the occurrence of DNA lesions. Induction of p21WAF is usually associated to the cell cycle control at the G1/S checkpoint; however, upregulation of p21WAF and induction of S-phase arrest it is not unprecedented and has been previously described in mouse fibroblasts treated with cisplatin, etoposide or mytomicin (Knudsen et al., 2000), in human melanocytes treated with thymidine dinucleotides (Pedeux et al., 1998), in human Saos-2 cells transduced with the p21WAF gene (Ogryzko et al., 1997) and in human cancer cell lines treated with 2,3 DCPE (2,3-dichlorophenoxy) propylamino-ethanol (Zhu et al., 2004).

Our data indicate that both compounds were highly cytotoxic in cancer cells while they were much less effective in Hacat immortalized keratinocytes. Indeed, Hacat keratinocytes can escape from the higginsianins-induced cytotoxic effect and resume growth after a lag or adaptation period. Remarkably, human primary keratinocytes appear to be totally insensitive to Higg A up to 10 μM and slightly affected by 10 μM Higg B. We can reasonably hypothesize that cells that fail to repair DNA damage are more sensitive to higginsianin effects. Accordingly, as assessed by MTT assay, the rescue of p53 wild type function in H1299 cancer cells decreased their sensitivity to a sublethal dose of Higg A or Higg B (Supplementary Fig. 1).

It is tempting to speculate that, unlike transformed cancer cells, healthy cells can still activate a checkpoint recovery pathway to overcome the higginsianin-induced cellular damage.

At present, however, we cannot exclude that higginsianins treatment, at higher doses or longer incubation times, may cause additional cellular damage at the membranes or cytoskeleton structure which are finally responsible for cell detachment. Given the absence of caspase-3 specific proteolytic cleavage of PARP1, we can conclude that higginsianins treated cells underwent non-apoptotic cell death. This cytotoxic effect contradicts earlier findings (8) that higginsianins induce cell death only in apoptosis proficient cells. On the basis of these results, higginsianins can be considered as attractive leads in the future development of novel potential anticancer agents.

Supplementary data to this article can be found online at https://doi.org/10.1016/j.tiv.2019.104614.

Declaration of Competing Interest

The authors declare no conflict of interest.

Acknowledgements

The work was carried out in part in the frame of Programme STAR 2017 financially supported by Università di Napoli Federico II and Compagnia di San Paolo. This work was supported by the Italian Association EEC Syndrome (AIEEC) and by the "*MIUR-DAAD Joint Mobility Program*" to Prof. Viola Calabrò.

The authors thank Dr. Maurizio Vurro of Istituto di Scienze delle Produzioni Alimentari, Consiglio Nazionale delle Ricerche, Bari, Italy for the supply of the mycelium of *C. higginsianum*. We thank Dr. Giuseppe Di Mauro for helping us with statistical analyses. Prof. A. Evidente is associated with the Istituto di Chimica Biomolecolare del CNR, Pozzuoli, Italy.

References

Amoresano, A., Di Costanzo, A., Leo, G., Di Cunto, F., La Mantia, G., Guerrini, L., Calabrò, V., 2010. Identification of ΔNp63α protein interactions by mass spectrometry. J. Proteome Res. 9 (4), 2042–2048. https://doi.org/10.1021/pr9011156.

Barbero, M., Artuso, E., Prandi, C., 2018. Fungal anticancer metabolites: synthesis towards drug discovery. Curr. Med. Chem. 25 (2), 141–185. https://doi.org/10.2174/0929867324666170511112815.

Bhanot, A., Sharma, R., Noolvi, M.N., 2011. Natural sources as potential anti-cancer agents: a review. Int. J. Phytomed. 3 (1), 09–26.

Cimmino, A., Masi, M., Evidente, M., Superchi, S., Evidente, A., 2015. Fungal phytotoxins with potential herbicidal activity: chemical and biological characterization. Nat. Prod. Rep. 32, 1629–1653. https://doi.org/10.1039/c5np00081e.

Cimmino, A., Mathieu, V., Masi, M., Baroncelli, R., Boari, A., Pescitelli, G., Ferderin, M., Lisy, R., Evidente, M., Tuzi, A., Zonno, M.C., Kornienko, A., Kiss, R., Evidente, A., 2016. Higginsianins A and B, two diterpenoid α-pyrones produced by *Colletotrichum higginsianum*, with in vitro cytostatic activity. J. Nat. Prod. 79 (1), 116–125. https://doi.org/10.1021/acs.jnatprod.5b00779.

di Martino, O., Troiano, A., Guarino, A.M., Pollice, A., Vivo, M., La Mantia, G., Calabrò, V., 2016. DNp63a controls YB-1 protein stability: evidence on YB-1 as a new player in keratinocyte differentiation. Genes Cells 21 (6), 648–660. https://doi.org/10.18632/oncotarget.140-51.

Evidente, A., Kornienko, A., Cimmino, A., Andolfi, A., Lefranc, F., Mathieu, V., Kiss, R., 2014. Fungal metabolites with anticancer activity. Nat. Prod. Rep. 31 (5), 617–627. https://doi.org/10.1039/c3np70078j.

Gagou, M.E., Zuazua-Villar, P., Meuth, M., 2010. Enhanced H2AX phosphorylation, DNA replication fork arrest, and cell death in the absence of Chk1. M.C.B. 21 (5), 739–752.

Garcia-Pajon, C.M., Isidro, G., 2003. Secondary metabolites isolated from *Colletotrichum* species. Nat. Prod. Rep. 20 (4), 426–431. https://doi.org/10.1039/b302183c.

Gulli, L.F., Palmer, K.C., Chen, Y.Q., Reddy, K.B., 1996. Epidermal growth factor-induced apoptosis in A431 cells can be reversed by reducing the tyrosine kinase activity. Cell Growth Differ. 7 (2), 173–178.

Hao, X., Pan, J., Zhu, X., 2013. Taxol producing fungi. In: Natural Products: Phytochemistry, Botany and Metabolism of Alcaloids, Phenolics and Terpenes, pp. 2797–2812.

Knudsen, K.E., Booth, D., Naderi, S., Sever-Chroneos, Z., Fribourg, A.F., Hunton, I.C., Knudsen, E.S., 2000. RB-dependent S-phase response to DNA damage. M.C.B. 20 (20), 7751–7763.

Lee, E.R., Kang, Y.J., Kim, J.H., Lee, H.T., Cho, S.G., 2005. Modulation of apoptosis in Hacat keratinocytes via differential regulation of ERK signaling pathway by flavonoids. J.B.C. 280 (36), 31498–31507. https://doi.org/10.1074/jbc.M505537200.

Lim, W., Park, J., Lee, Y.H., Hong, J., Lee, Y., 2015. Subglutinol A, an immunosuppressive a-pyrone diterpenoid from *Fusarium subglutinans*, acts as an estrogen receptor antagonist. BBRC 461 (3), 507–512. https://doi.org/10.1016/j.bbrc.2015.04.053.

Masi, M., Zonno, M.C., Cimmino, A., Reveglia, P., Berestetskiy, A., Boari, A., Vurro, M., Evidente, A., 2018. On the metabolites produced by *Colletotrichum gloeosporioides* a fungus proposed for the *Ambrosia artemisiifolia* biocontrol; spectroscopic data and absolute configuration assignement of colletochlorin A. Nat. Prod. Res. 32 (13), 1537–1547. https://doi.org/10.1080/14786419.2017.1385020.

Masi, M., Freda, F., Sangermano, F., Calabrò, V., Cimmino, A., Cristofaro, M., Meyer, S., Evidente, A., 2019. Radicinin, a fungal phytotoxin as a target-specific bioherbicide for invasive buffelgrass (*Cenchrus ciliaris*) control. Molecules 24 (6). https://doi.org/10.3390/molecules24061086.

Mejia-Ramirez, E., Limbo, O., Langerak, P., Russel, P., 2015. Critical function of γH2A in S-phase. PLoS Genet. 11 (9), e1005517.

Ogryzko, V.V., Wong, P., Howard, B.H., 1997. WAF1 retards S-phase progression primarily by inhibition of cyclin-dependent kinases. M.C.B. 17 (8), 4877–4882.

Pedeux, R., Al-Irani, N., Marteau, C., Pellicier, F., Branche, R., Ozturk, M., Doré, J.F., 1998. Thymidine dinucleotides induce S phase cell cycle arrest in addition to increased melanogenesis in human melanocytes. J. Investig. Dermatol. 111 (3), 472–477.

Reiss, M., Brash, D.E., Munoz-Antonia, T., Simon, J.A., Ziegler, A., Vellucci, V.F., Zhou, Z.L., 1992. Status of the p53 tumor suppressor gene in human squamous carcinoma cell lines. Oncol. Res. 4 (8–9), 349–357.

Rogakou, E.P., Pilch, D.R., Orr, A.H., Ivanova, V.S., Bonner, W.M., 1998. DNA double-stranded breaks induce histone H2AX phosphorylation on serine 139. J.B.C. 273 (10), 5858–5868.

Savic, V., Yin, B., Maas, N.L., Bredemeyer, A.L., Carpenter, A.C., Helmink, B.A., Yang-lott, K.S., Sleckmann, B.P., Bassing, C.H., 2009. Formation of dynamic gamma-H2AX domains along broken DNA strands is distinctly regulated by ATM and MDC1 and dependent upon H2AX densities in chromatin. Mol. Cell 34 (3), 298–310. https://doi.org/10.1016/j.molcel.2009.04.012.

Sherr, C.J., Roberts, J.M., 1999. CDK inhibitors:positive and negative regulators of G1-phase progression. Genes Dev. 13 (12), 1501–1512.

Slovackova, J., Smarda, J., Smardova, J., 2012. Roscovitine-induced apoptosis of H1299 cells depends on the functional status of p53. Neoplasma 59 (6), 606–612. https://doi.org/10.4149/neo_2012_077.

Soldani, C., Scovassi, A.I., 2002. Poly(ADP-ribose) polymerase-1 cleavage during apoptosis: an update. Apoptosis 7 (4), 321–328.

Vivo, M., Di Costanzo, A., Fortugno, P., Pollice, A., Calabrò, V., La Mantia, G., 2009. Downregulation of ΔNp63α in keratinocytes by p14ARF-mediated SUMO-conjugation and degradation. Cell Cycle 8 (21), 3545–3551. https://doi.org/10.4161/cc.8.21.9954.

Vivo, M., Matarese, M., Sepe, M., Di Martino, R., Festa, L., Calabrò, V., La Mantia, G., Pollice, A., 2015. MDM2-mediated degradation of p14ARF: A novel mechanism to control ARF levels in cancer cells. PLoS ONE 10 (2). https://doi.org/10.1371/journal.pone.0117252.

Vivo, M., Fontana, R., Ranieri, M., Capasso, G., Angrisano, T., Pollice, A., Calabrò, V., La Mantia, G., 2017. p14ARF interacts with the focal adhesion kinase and protects cells from anoikis. Oncogene 36, 4913–4928. https://doi.org/10.1038/onc.2017.104.

Zhu, H., Zhang, L., Wu, S., Teraishi, F., Davis, J.J., Jacob, D., Fang, B., 2004. Induction of S-phase arrest and p21overexpression by a small molecule [[3-(2,3-dichlorophenoxy) propyl]amino] ethanol in correlation with activation of ERK. Oncogene 23 (29), 4984. https://doi.org/10.1038/sj.onc.1207645.